DOI: 10.1002/ejoc.200700906

Metathesis Reactions of Formaldehyde Acetals – Experimental and Computational Investigation of Isomeric Families of Cyclophanes under Dynamic Conditions

Roberta Cacciapaglia,[a] Stefano Di Stefano,[a] Luigi Mandolini,*[a] Paolo Mencarelli,*[a] and Franco Ugozzoli*[b]

Dedicated to Professor David N. Reinhoudt on the occasion of his 65th birthday

Keywords: Cyclooligomerization / Dynamic covalent chemistry / Effective molarity / Molecular modeling / Transacetalation

The acid-catalyzed transacetalation of cyclophane formaldehyde acetals incorporating *m*-xylylene units (***m*-C$_i$**) generates a well behaved dynamic library of oligomeric macrocycles. Effective Molarities (*EM*) relating to the formation of the lower cyclic oligomers (i = 2–4) were estimated from equilibrium concentrations measured under conditions closely approaching the critical monomer concentration. Comparison with available *EM* data relating to the formation of the isomeric paracyclophanes ***p*-C$_i$** shows that the metacyclophanes ***m*-C$_i$** are considerably more stable, the stability difference being particularly significant for i = 2. Molecular modeling indicated that incorporation of COCOC moieties in the cyclic structures enforces deviations from the most stable g^+g^+/g^-g^- conformation. Consistently with experimental results, such deviations are at a maximum for the dimeric paracyclophane ***p*-C$_2$**, and tend to decrease with increasing ring size in both series. Molecular modeling also showed that the stability of the heterodimer ***m,p*-C$_2$** is comparable to that of ***m*-C$_2$**, which is again in agreement with the results of a cross-experiment in which a mixture of ***m*-C$_2$** and ***p*-C$_2$** was allowed to equilibrate.

Introduction

A major motivation for the current wide interest in reactions involving covalent bond formation under fully reversible conditions[1] has been the prospect of the unexpected choice of receptors by guest molecules (templates) by virtue of the "proof reading and editing" capability of Dynamic Covalent Chemistry (DCC). In this paper we focus on another important, still overlooked, potential of DCC. Whenever reversible macrocyclization processes are considered, DCC turns out to be a most convenient source of information about the thermodynamic stability of the interconverting macrocycles, which is hardly ever accessible from other sources, given the general paucity of thermodynamic data for ring compounds over large ring size ranges. In fact, the only extensive series of ring compounds for which strain energies are available are the cycloalkanes[2] up to ring 16 and the lactones[3] up to ring 14. Standard heats of formation ($\Delta H_f°$) for other ring sizes are limited to scattered examples.[4] The situation for standard entropy ($S°$) is even worse.

We recently reported on the fully reversible interchange of paracyclophane formaldehyde acetals ***p*-C$_i$** (Scheme 1) through acid-catalyzed transacetalation in chloroform.[5] Peculiar structural properties were found for the lower cyclic oligomers ***p*-C$_2$** to ***p*-C$_5$**, due to the constraints imposed by the cyclic arrangement on the C–O–C–O–C chain, which has highly demanding conformational requirements.[5a] A strain energy of 3.3 kcal mol^{-1} was assigned to the 18-membered dimer ***p*-C$_2$**, an exceedingly high value for a ring of that size. Even more surprising was the strain energy of 1.3 kcal mol^{-1} estimated for the 45-membered pentamer ***p*-C$_5$**, in contrast to the common view that rings with more than 25–30 skeletal atoms are virtually strainless.

To investigate the stability of macrocycles incorporating COCOC chains further, we have extended our previous study (Scheme 1) to the acid-catalyzed transacetalation of cyclophane formals ***m*-C$_i$**, featuring *m*-xylylene spacers.

[a] IMC CNR Sezione Meccanismi di Reazione Dipartimento di Chimica, Sapienza Università di Roma,
P.le A. Moro 5, Box 34, Roma 62, 00185 Roma, Italy
Fax: +39-06-490421
E-mail: luigi.mandolini@uniroma1.it
paolo.mencarelli@uniroma1.it
[b] Dipartimento di Chimica Generale ed Inorganica, Chimica Analitica, Chimica Fisica, Università di Parma
V.le G. P. Usberti 17/a, 43100 Parma, Italy
Fax: +39-0521-905557
E-mail: franco.ugozzoli@unipr.it

Supporting information for this article is available on the WWW under http://www.eurjoc.org or from the author.

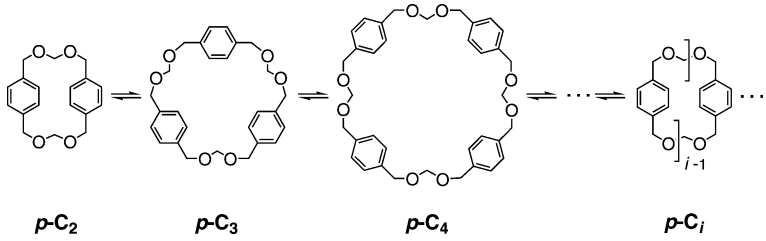

Scheme 1. Ring-ring equilibria of cyclophane formals ***p*-C$_i$**.

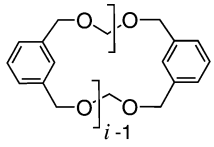

A parallel computational study, based on molecular mechanics and molecular dynamics calculations, was carried out to provide more insights into the factors that rule the relative stabilities of para- and metacyclophane formals, and to predict the outcomes of cross-transacetalation experiments. X-ray crystal structures of ***p*-C$_2$** and ***m*-C$_2$** dimers were compared with the results from computational studies.

Results and Discussion

Pure samples of the lower metacyclophane oligomers ***m*-C$_2$** to ***m*-C$_5$** were obtained from the irreversible reaction between benzene-1,3-dimethanol and bromochloromethane in the presence of NaH in boiling THF under Ziegler's high-dilution conditions [Equation (1)]. Yields of the lower oligomers (10% ***m*-C$_2$**; 6% ***m*-C$_3$**; 6% ***m*-C$_4$**) were higher than those previously reported[5a] for the *para* analogues (1.2% ***p*-C$_2$**; 3.7% ***p*-C$_3$**; 2.7% ***p*-C$_4$**) under virtually identical conditions, which provides an indication of lower strain energies in the *meta* series.

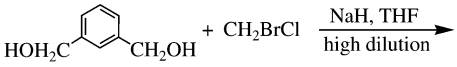

$$\longrightarrow \textbf{\textit{m}-C}_2 + \textbf{\textit{m}-C}_3 + \textbf{\textit{m}-C}_4 + \textbf{\textit{m}-C}_5 + \text{higher oligomers /polymer} \quad (1)$$

As also previously observed for the *para* series,[5a] no trace of the monomeric ring ***m*-C$_1$** was found, showing that the five-atom COCOC chain is too short to span the *m*-phenylene spacer.

A set of acid-catalyzed transacetalation experiments were carried out on ***m*-C$_2$** solutions in $CDCl_3$ at 25 °C, at varying reactant concentrations in the range of 10 to 200 mM. The ring-opening cyclooligomerization processes, generating the whole library of interconverting macrocycles, were initiated by the addition of a catalytic amount of triflic acid (TfOH). Equilibration was complete within 4–5 h. ^{1}H NMR spectra (OCH_2O signals) of equilibrated mixtures are shown in Figure 1. Signal assignments were based on the ^{1}H NMR spectra of pure samples of ***m*-C$_2$** to ***m*-C$_5$**, and on a combination of ^{1}H NMR and ESI-MS spectra of chromatographic fractions containing higher oligomeric materials. Whereas the equilibrium concentrations of ***m*-C$_2$** could be determined with the ordinary accuracy of integrated ^{1}H NMR peak intensities, the deconvolution procedure adopted for ***m*-C$_3$** afforded integrated intensities of only moderate accuracy, particularly in the high-concentration region. The situation was even worse for ***m*-C$_4$**, for which the determined concentrations are to be taken as semiquantitative estimates at best. Plots of the equilibrium molar concentrations of ***m*-C$_2$** to ***m*-C$_4$** against total monomer concentration $[M]_{tot}$ (Figure 2) display a tendency toward saturation in the high-concentration region.

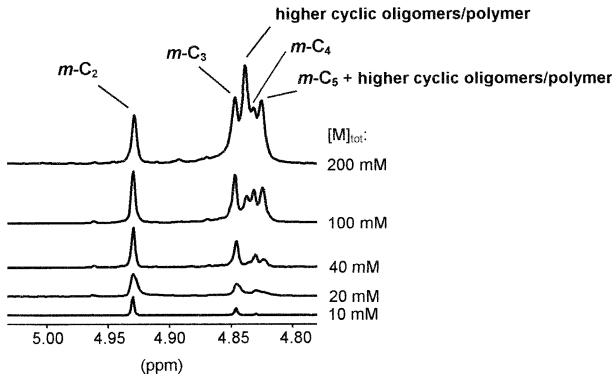

Figure 1. ^{1}H NMR spectra (OCH_2O signals) of equilibrated solutions obtained in the acid-catalyzed transacetalation of ***m*-C$_2$**, at the given equivalent monomer concentration $[M]_{tot}$, ($CDCl_3$, 25 °C).

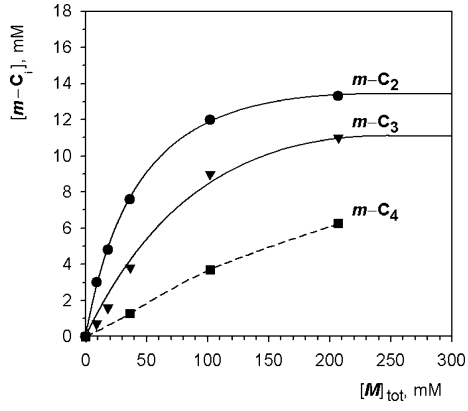

Figure 2. Equilibrium concentration of ***m*-C$_2$** to ***m*-C$_4$** from acid-catalyzed transacetalation of ***m*-C$_2$**, as a function of the total monomer concentration $[M]_{tot}$ ($CDCl_3$, 25 °C).

Such a behavior is in keeping with Jacobson and Stockmayer's theory of macrocyclization equilibria, according to which the concentration of each individual cyclic species increases with increasing monomer concentration, until a critical value is reached.[6] Above such a critical value, the concentration of each cyclic species remains constant, and coincides with the effective molarity (EM_i) of the given cyclic oligomer $\mathbf{C}_i$: $EM_i = (K_{intra})_i/K_{inter}$. The quantities K_{inter} and $(K_{intra})_i$ are defined in Equations (2) and (3), respectively, where **P** denotes linear polymer chains. As pointed out by Flory,[7] the chemical nature of end groups is immaterial to the argument. For simplicity the end groups may be regarded as free radicals, such as in the hypothetical linear oligomer $\mathbf{P}_i$.

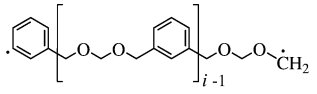

$\mathbf{P}_i$

Combination of Equation (2) with Equation (3) leads to the ring/chain equilibrium of Equation (4), with $EM_i \equiv (K_{intra})_i/K_{inter} = [\mathbf{C}_i]\,[\mathbf{P}_{j-i}]/[\mathbf{P}_j]$.[8]

$$\mathbf{P}_j \underset{K_{inter}}{\rightleftharpoons} \mathbf{P}_i + \mathbf{P}_{j-i} \quad (2)$$

$$\mathbf{P}_i \overset{(K_{intra})_i}{\rightleftharpoons} \mathbf{C}_i \quad (3)$$

$$\mathbf{P}_j \rightleftharpoons \mathbf{C}_i + \mathbf{P}_{j-i} \quad (4)$$

Jacobson–Stockmayer theory shows that when the extent of reaction (p) in the linear fraction is very close to 1,[9] Equation (4) reduces to a sufficient approximation to the useful form of Equation (5),

$$EM_i \approx [\mathbf{C}_i] \quad (5)$$

according to which the equilibrium concentration of a given cyclic oligomer provides a direct measure of its EM on the condition that measurements are carried out at monomer concentration above the critical value.

A major problem with the equilibrium concentrations plotted in Figure 2 is that they do not allow the critical monomer concentration to be determined with any precision. Extrapolation of [***m*-C$_2$**] to infinite monomer concentration in a plot of [***m*-C$_2$**] against $1/[M]_{tot}$ (Figure 3) gave a value of 15 mM for the limiting concentration of ***m*-C$_2$**, very close to the value of 13 mM determined at $[M]_{tot}$ = 200 mM. This indicates that the highest monomer concentration in the equilibration experiments closely approaches the critical value. With use of the presumably more precise analytical concentrations of ***m*-C$_3$** measured in the more dilute runs, a value of 31 M^{-1} was calculated for the equilibrium constant $K_{2,3}$; see Equation (6), $K_{2,3} = [\textit{m}\text{-}\mathbf{C}_3]^2/[\textit{m}\text{-}\mathbf{C}_2]^3$).

$$3\,\textit{m}\text{-}\mathbf{C}_2 \overset{K_{2,3}}{\rightleftharpoons} 2\,\textit{m}\text{-}\mathbf{C}_3 \quad (6)$$

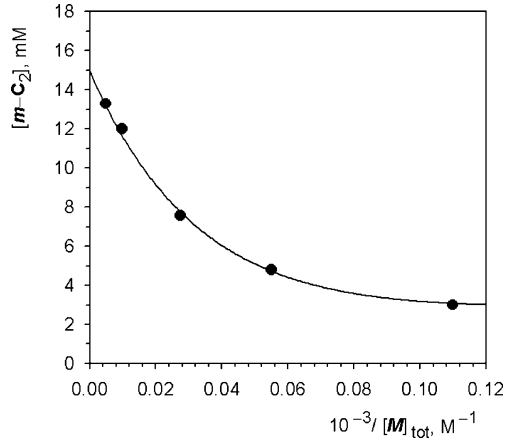

Figure 3. Extrapolation of equilibrium concentrations of ***m*-C$_2$** (from Figure 2) to infinite monomer concentration.

Combination of the value of $K_{2,3}$ with that of the limiting concentration of ***m*-C$_2$** (15 mM) gave a value of 10 mM for the limiting concentration of ***m*-C$_3$**, again showing that the experiment carried out at $[M]_{tot}$ = 200 mM closely approaches saturation conditions. In view of the presumably large errors affecting the equilibrium concentrations of ***m*-C$_4$**, any refinement of experimental data appeared inappropriate. Hence the concentration of 6 mM measured at the highest monomer concentration was taken as a rough estimate of the limiting concentration of ***m*-C$_4$**.

The EM_i values relating to the formation of the metacyclophane oligomers ***m*-C$_i$** (i = 2–4) are compared with the corresponding values of the paracyclophanes ***p*-C$_i$** in Table 1. It is apparent that the EMs in the *meta* series are significantly higher than the corresponding values in the *para* series. The ring strain energies (E_{strain}) reported in

Table 1. Experimentally determined EM_i values and calculated strain energies in ***m*-C$_i$** and ***p*-C$_i$** series.

		***m*-C$_i$**			***p*-C$_i$**[a]	
i	Ring atoms	EM_i^S (M) [b]	EM_i (M) [c]	Strain energy [d] [kcal mol^{-1}]	EM_i (M)	Strain energy [kcal mol^{-1}]
2	18	8.5×10^{-2}	1.5×10^{-2}	1.0	3.0×10^{-4}	3.3
3	27	1.6×10^{-2}	1.0×10^{-2}	ca. 0.3	9.0×10^{-4}	1.7
4	36	7.0×10^{-3}	ca. 6×10^{-3}	≈ 0	5.9×10^{-4}	1.5

[a] Data from ref.[5a]. [b] Taken from the compilation of entropic components of EM (EM^S) as a function of the number r of rotatable bonds reported in Table 1 of ref.[10b]. For the present system $r = 6i - 1$. The listed EM_i^S data have been corrected for the symmetry number of C_i: namely, $\sigma_I = 2i$. [c] Estimated errors range between ±5% (***m*-C$_2$**) and ±20% (***m*-C$_4$**). [d] Calculated at 298 K as $RT\ln(EM_i^S/EM_i)$.

Table 1 were estimated with reference to Equation (7). The second term on the right of Equation (7) defines the entropy component (EM^S) of the *EM* [Equation (8)].

$$EM_i = \exp\left(-\frac{\Delta H_{intra} - \Delta H_{inter}}{RT}\right)\exp\left(\frac{\Delta S_{intra} - \Delta S_{inter}}{R}\right) \quad (7)$$

$$EM^S = \exp\left(\frac{\Delta S_{intra} - \Delta S_{inter}}{R}\right) \quad (8)$$

Whenever strainless rings are formed ($\Delta H_{intra} = \Delta H_{inter}$), the *EM* is determined solely by the entropic component EM^S, which is largely independent of the nature of end groups, because of a substantial cancellation of contributions due to chemical changes in the ($\Delta S_{intra} - \Delta S_{inter}$) quantity. However, it strongly depends on the conformational (torsional) entropy loss suffered by the chain precursors upon cyclization. It was found that, to a useful approximation, the magnitude of ($\Delta S_{intra} - \Delta S_{inter}$) is solely determined by the number *r* of essential single bonds in the chain precursors. The EM^S values in Table 1, taken from the compilation of EM^S values as a function of *r*,[10] were combined with the experimentally determined *EM* values to calculate E_{strain} for the various rings according to Equation (9).[11]

$$E_{strain} \equiv (\Delta H_{intra} - \Delta H_{inter}) = RT \ln \frac{EM^S}{EM} \quad (9)$$

A strain energy value of 1.1 kcal mol^{-1} was calculated for the dimer ***m*-C$_2$**, whereas the trimer ***m*-C$_3$** and the tetramer ***m*-C$_4$** turned out to be virtually strainless. A striking different picture was previously observed for the *para* isomers,[5a] as shown by the corresponding data reported in Table 1 for comparison. The origin of the relatively high strain energies of the paracyclophanes ***p*-C$_i$** was ascribed[5a] to the torsional strain arising from deviations of the COCOC chain from the most stable g^+g^+/g^-g^- conformation.[12] Given that the latter corresponds to a narrow and deep energy well, a significant torsional strain is introduced whenever the geometrical constraints imposed by a cyclic arrangement cause even small deviations from the optimal geometry. The geometrical constraints imposed by the *m*-phenylene spacers turn out to be much less severe than those imposed by the *p*-phenylene spacers. Not surprisingly, in both series, such geometrical constraints become less stringent as the ring size gets larger.

X-ray Crystal Structures

Single crystals of ***p*-C$_2$** and ***m*-C$_2$** suitable for X-ray analysis were obtained by slow evaporation of solutions of the pure compounds in a solvent mixture of dichloromethane/heptane/acetone (11:8:0.7, v/v). The molecular structures of the two macrocycles are illustrated in Figure 4 (parts a and b), together with the values of the torsion angles along the two COCOC chains connecting the aromatic rings, showing that in both cases the chains adopt conformations resembling the g^+g^+/g^-g^- arrangements. The main significant difference between the two structures is the reciprocal orientation of the two aromatic rings.

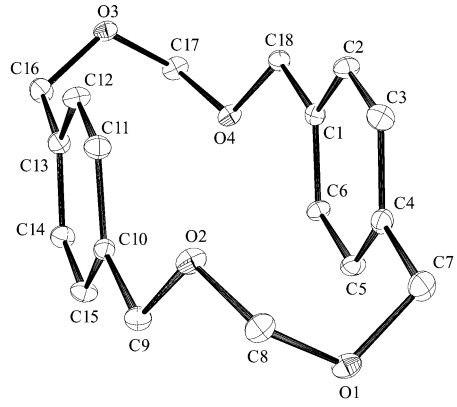

(a) **C4-C7-O1-C8** –80.65(8), **C7-O1-C8-O2** 71.90(8), **O1-C8-O2-C9** 70.03(8), **C8-O2-C9-C10** –159.95(6), **C1-C18-O4-C17** 158.23(6), **C18-O4-C17-O3** –69.2(1), **O4-C17-O3-C16** –68.60(9), **C17-O3-C16-C13** 75.38(9)

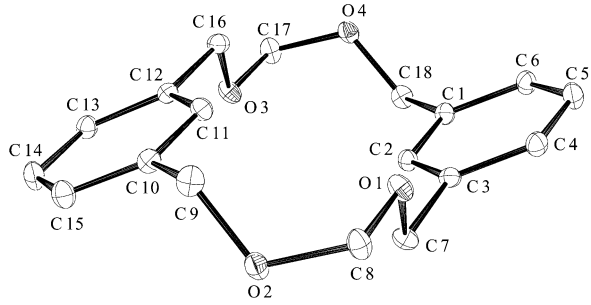

(b) **C1-C18-O4-C17** –115.8(4), **C18-O4-C17-O3** 72.9(4), **O4-C17-O3-C16** 64.7(4), **C17-O3-C16-C12** 178.1(3), **C3-C7-O1-C8** –177.5(3), **C7-O1-C8-O2** –67.4(4), **O1-C8-O2-C9** –70.9(4), **C8-O2-C9-C10** 117.3(4)

Figure 4. ORTEP drawings of the molecular structures with relevant torsion angles (°): a) *para* dimer ***p*-C$_2$** and b) *meta* dimer ***m*-C$_2$**. The hydrogen atoms have been omitted for clarity.

In both cases the opposite rings are in the "slipped parallel" geometry [the dihedral angles between least-squares planes are 0.50(3)° in ***p*-C$_2$** and 0.3(1)° in ***m*-C$_2$**], but the horizontal shift (*H*) and the vertical separation (*V*) between planes in the two structures are quite different. In ***p*-C$_2$** (Figure 4, a) the two rings are almost superimposed in a face-to-face fashion (H = 1.39, V = 3.51 Å), whereas those in ***m*-C$_2$** (Figure 4, b) are significantly shifted with respect to one another (H = 5.84, V = 2.95 Å).

The mutual arrangement of the aromatic nuclei suggests a reasonable explanation for the widely different affinities of the two isomeric dimers toward silver(I) cation. The ability of ***p*-C$_2$** to bind strongly to Ag^+ has been reported previously.[5a] The X-ray crystal structure of the $(CF_3SO_2)_2$-NAg complex of ***p*-C$_2$**, obtained by slow evaporation of an equimolar chloroform solution of the components, is shown in Figure 5. Two different units of the complex were found in the crystal lattice. In both the complexes the metal ion is paired to the $(CF_3SO_2)_2N^-$ counteranion; the complex has a C_2 symmetry and the Ag–N bond lies on a twofold symmetry axis (Figure 5). There are also similarities between

the two complexes in the coordination spheres of the metal ions. In both complexes the Ag^+ cation is coordinated to two opposite oxygen atoms of the COCOC chains (O1a and its symmetry-related oxygen in the Ag2 complex; O2c and its symmetry-related oxygen in the Ag1 complex) and to two opposite sets of η^3 Ag^+–C bonds with the carbon atoms of the two opposite aromatic rings (C1a, C2a, C3a, and their symmetry-related ones in the Ag2 complex; C4c, C5c, C6c, and their symmetry-related ones in the Ag1 complex).

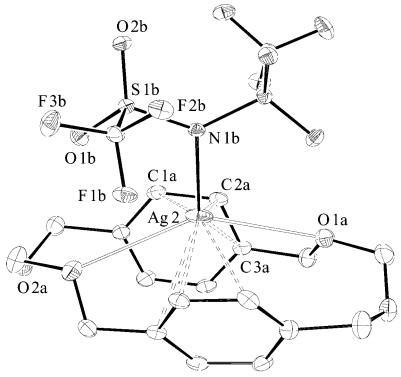

(a) **Ag2-O1a** 3.007(5), **Ag2-C1a** 2.711(9), **Ag2-C2a** 2.442(8), **Ag2-C3a** 2.932(7), **Ag2-N1b** 2.369(6)

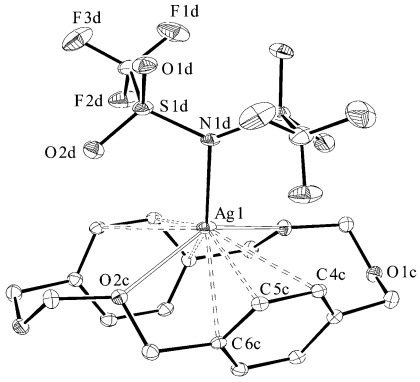

(b) **Ag1-O2c** 2.705(4), **Ag1-C4c** 2.890(4), **Ag1-C5c** 2.503(5), **Ag1-C6c** 2.859(5), **Ag1-N1d** 2.344(6)

Figure 5. ORTEP drawings of the molecular structures of the two independent units of the complex of ***p*-C_2** with $(CF_3SO_2)_2NAg$ with relevant bond lengths (Å). The hydrogen atoms have been omitted for clarity.

However, the bond lengths in the coordination spheres of the two Ag^+ ions (Figure 5) show that in spite of these rough similarities, the binding of the silver cation to the macrocycle is substantially different in the two complexes. In one complex unit (Figure 5, a) the η^3 Ag^+–C bonds are stronger and the Ag^+–O bonds weaker than in the other complex (Figure 5, b). The average Ag2–C distance for the η^3 bonds [2.695(8) Å] is significantly shorter than the average Ag1–C distance [2.763(5) Å] in the other complex unit. Nevertheless, the weaker η^3 binding of the macrocycle to the $Ag1^+$ ion is compensated by the stronger Ag^+–O bonds: Ag1–O2c [2.705(4) Å] is significantly shorter than the corresponding Ag2–O1a bond length of 3.007(5) Å in the other complex unit. Although long, the latter bond is decidedly shorter than the longest Ag–O bond (3.164 Å) found in the Cambridge Crystallographic Data Base.[13]

The self-assembly of the two complex units in the crystal lattice is also assisted by weak attractive intermolecular interactions. An intermolecular F1b···C6c contact of 3.113(7) Å, shorter than the sum of the van der Waals radii, links the fluorine atom F1b of the counteranion in the Ag2 complex unit to the carbon atom C6c of the macrocycle in the Ag1 complex unit. Thus, in the crystal lattice, the two independent complex units are piled up in separated columnar arrangements, parallel to the crystallographic *c* axis as illustrated in Figure 1S (see electronic supporting information).

In marked contrast with the behavior of ***p*-C_2**, no significant evidence of complexation was found for ***m*-C_2**,[14] showing that simultaneous complexation of the silver cation with both aromatic rings is a prerequisite for effective binding.

Computational Procedure and Results

Molecular mechanics and dynamics calculations were carried out with the force field MMFF[15] as implemented in the Macromodel® 6.0 molecular modeling system.[16] The MMFF force field was chosen because it is considered one of the most reliable force field when compared to others available.[17]

A conformational research by the Monte-Carlo-based Low-Mode Conformational Search method was carried out for each cyclophane.[18] The length of each search was of 5000, 10000, and 15000 steps for the dimers, trimers, and tetramers, respectively. Only structures with steric energies in the 12 kJ mol^{-1} (2.87 kcal mol^{-1}) range above the global minimum were collected. To confirm that the global minimum was indeed found, for each cyclophane a new search was carried out by using the Monte Carlo Multiple Minimum Conformational Search method.[19] This new search, of the same length as the previous one, was started from a different structure and with a different seed number. In all cases, for each cyclophane, the two alternative searches provided the same global minimum.

It is interesting to compare the structures of the two global minima found for the *para* and *meta* dimers (Figure 6) with the corresponding experimentally observed X-ray structures of the two isomers in the solid state (Figure 4). The structure of the global minimum found for the *meta* dimer ***m*-C_2** is very similar to the X-ray structure in that both show the g^+g^+/g^-g^- conformation for the two COCOC moieties. The structure of the global minimum found for the *para* dimer ***p*-C_2** instead shows the g^+a/g^+a conformation for the COCOC moieties. The first conformer that shows the same g^+g^+/g^-g^- pattern found in the X-ray structure, is 1.35 kcal mol^{-1} above the global minimum, thus suggesting that the cyclic arrangement introduces highly demanding geometrical constraints in the paracyclophane dimer, and enforces a deviation from the intrinsically most stable g^+g^+/g^-g^- arrangement of the acyclic analogue.

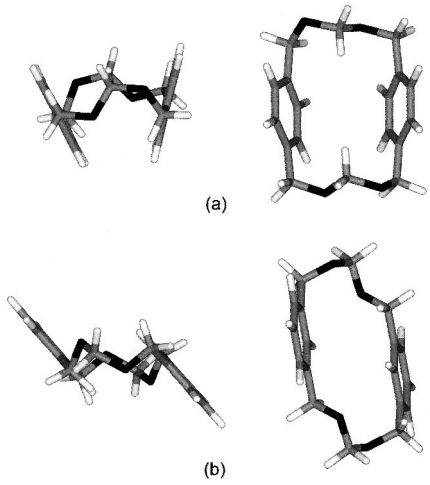

Figure 6. Side views and top views of the global minimum structures found for a) the *para* dimer ***p*-C$_2$** and b) the *meta* dimer ***m*-C$_2$**.

As to the steric energies obtained from the simulation, we had to take into account that each cyclophane is actually described by several conformations. The number of conformations found for each cyclophane in the 12 kJ mol^{-1} range above the global minimum varies from tens for dimers to hundreds for trimers and tetramers. Consequently, it is still manageable to obtain the Boltzmann averaged steric energies for ***m*-C$_2$** and ***p*-C$_2$**, but not for higher oligomers. Therefore the relative stabilities of the cyclophanes were evaluated on the basis of the average potential energy ($<E>$) obtained from a constant temperature (298 K) molecular dynamics simulation started from the global minimum of each cyclophane. After an equilibration run of 250 ps, the length of the production runs were 1, 1.5, and 2.0 ns for dimers, trimers, and tetramers, respectively. It was verified that the production runs were long enough to obtain convergence for the average potential energy ($<E>$) to the first decimal digit. For each cyclophane the molecular dynamics simulation was repeated twice and identical results were obtained.

The average potential energy ($<E>$) calculated for a given ring is not directly comparable to the strain energy (E_{strain}), because the two quantities are based on different reference systems. The energy differences listed in Table 2, however, are closely comparable, because, being ***p*-C$_i$** and ***m*-C$_i$** isologous molecules,[20] differences due to the different reference systems are cancelled out.

It is apparent that the $\Delta<E>$ [*para* – *meta*] values calculated for the dimers and tetramers exceed the corresponding ΔE_{strain} values by sizeable amounts. However, apart from the discrepancies emerging from a comparison of exact figures, it should be stressed that the calculated $\Delta<E>$ [*para* – *meta*] quantities are always positive, which is in agreement with the finding that paracyclophanes ***p*-C$_i$** (i = 2–4) are less stable than the corresponding metacyclophanes ***m*-C$_i$**. Furthermore, the normalized $<E>$ values (Table 2) decrease regularly from dimer to tetramer in both series, in good agreement with the observed trends of strain energies (Table 1).

Table 2. Calculated average potential energy ($<E>$) values (scaled at 298 K) for macrocycles ***p*-C$_2$** to ***p*-C$_4$** and ***m*-C$_2$** to ***m*-C$_4$**. Differences of average potential energy values and strain energy values for the two isomers of cyclooligomers **C$_2$**–**C$_4$**. All energies in kcal mol^{-1}.

	$<E>$[a]	$\Delta<E>$ [*para* – *meta*]	ΔE_{strain} [*para* – *meta*][b]
***p*-C$_2$**	68.1 (34.05)	3.7	2.3
***m*-C$_2$**	64.4 (32.20)		
***p*-C$_3$**	96.6 (32.20)	1.5	1.4
***m*-C$_3$**	95.1 (31.70)		
***p*-C$_4$**	127.1 (31.77)	2.2	1.4
***m*-C$_4$**	124.9 (31.22)		

[a] The $<E>$ values normalized for the number of monomers in each macrocycle are reported in parentheses. [b] Calculated as $(\Delta E_{strain})_i = (E^{para}_{strain})_i - (E^{meta}_{strain})_i = RT\ln(EM_i^{meta}/EM_i^{para})$ from data in Table 1.

We therefore conclude that the computational procedure used in this work is a useful tool for an easy and relatively fast assessment, at least on a semiquantitative basis, of the stability of macrocyclic formaldehyde acetals.

As a further, independent test of the reliability of our computational model, it was used to predict the outcome of a dynamic combinatorial experiment involving an acid-catalyzed cross-transacetalation of isomeric cyclophane formaldehyde acetals, as reported in the next section.

An Acid-Catalyzed Transacetalation Cross-Experiment

A system composed of two different building blocks offers a higher degree of complexity, as heteroaggregates are also formed together with the homoaggregates. In a dynamic library derived from a mixture of ***m*-C$_2$** and ***p*-C$_2$** building blocks, the simplest of such heteroaggregates is the mixed dimer ***m*,*p*-C$_2$** [Equation(10)].

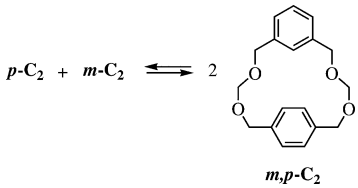

(10)

Although no theory of macrocyclization equilibria of systems composed of two or more building blocks is yet available, there is no doubt that the relative abundances of the isologous macrocycles ***m*-C$_2$**, ***p*-C$_2$**, and ***m*,*p*-C$_2$** at equilibrium must be related to their thermodynamic stabilities.

The heterodimer ***m*,*p*-C$_2$** was subjected to the computational procedure described above. Figure 7 shows all the conformations found in the conformational search within a 1 kcal mol^{-1} range above the global minimum.[21] Comparison of a value of 65.1 kcal mol^{-1} calculated for the average potential energy ($<E>$) of ***m*,*p*-C$_2$** with those of 68.1 and 64.4 kcal mol^{-1} obtained for ***p*-C$_2$** and ***m*-C$_2$**, respectively, shows that the heterodimer is definitely more stable than ***p*-C$_2$**, and has a stability comparable to that of ***m*-C$_2$**.[22]

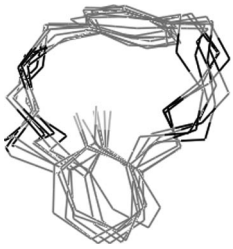

Figure 7. Low-energy conformations of ***m,p*-C_2** (up to a 1 kcal mol^{-1} range above the global minimum: i.e. 85% of the total conformational population) generated in the conformational search. The hydrogen atoms are omitted for clarity, except for that responsible for the ^{1}H NMR signal at δ = 5.45 ppm (see ref.[21]).

The cross ring-opening cyclooligomerization of an equimolar mixture of ***p*-C_2** and ***m*-C_2** [12.5 mM each, $(p\text{-}M)_{tot}$ + $(m\text{-}M)_{tot}$ = 50 mM] in $CDCl_3$ at ambient temperature was initiated by the addition of TfOH (0.4 mM). Equilibrium was reached after 5 h. The aliphatic region of the ^{1}H NMR spectrum of the reaction mixture at time zero (trace *a*) and of the equilibrated mixture (trace *b*) are reported in Figure 8. Trace *b* shows that a large fraction of the starting materials is in the form of unidentified higher oligomers, and that the concentrations of ***m*-C_2** and ***m,p*-C_2**[23] are 1.5 and 5.8 mM, respectively, whereas no trace of ***p*-C_2** ([***p*-C_2**] < 0.05 mM) is visible. It appears therefore that the results of the cross-equilibration experiments are in substantial agreement with the computational results, in that the stability of the heterodimer ***m,p*-C_2** is comparable to that of ***m*-C_2**, and decidedly higher than that of ***p*-C_2**.

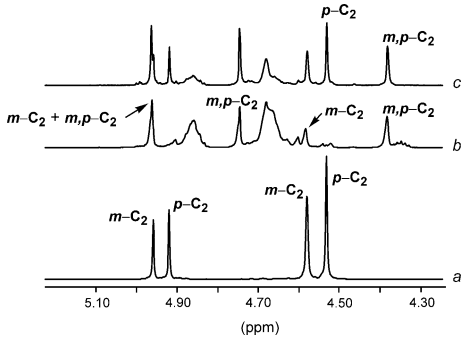

Figure 8. Aliphatic region of ^{1}H NMR spectra of *a*) an equimolar solution (12.5 mM each) of ***p*-C_2** and ***m*-C_2** before the addition of TfOH; *b*) the equilibrated solution after 5 h from the addition of TfOH; *c*) solution of trace *b* after the reequilibration in the presence of $(CF_3SO_2)_2NAg$ and extraction with ammonia.

We have already pointed out that ***p*-C_2**, unlike ***m*-C_2**, is an effective binder of Ag^+ ion, because its conformation allows simultaneous interaction of both aromatic rings with the metal ion. A glance at the low-energy conformations of ***m,p*-C_2** (Figure 7) suggests that the heterodimer should be a very poor candidate for an effective complexation of Ag^+ ion.

The dynamic library obtained in the cross-experiment (Figure 8, trace *b*), was treated with excess solid $(CF_3SO_2)_2$-NAg. The new equilibrium composition revealed by the ^{1}H NMR spectrum (Figure 8, trace *c*) is [***p*-C_2**] = 4.9 mM, [***m,p*-C_2**] = 9.0 mM, [***m*-C_2**] = 2.9 mM, showing that two-thirds of the material is now distributed among the dimeric rings. Comparison with trace *b* shows that the silver template amplifies the concentration of ***p*-C_2** by no less than 100-fold, whereas the amplification factors for ***m*-C_2** and ***m,p*-C_2** hardly amount to a factor of 2. These findings are clearly consistent with the view that not only ***m*-C_2**, but also ***m,p*-C_2** should be a very poor binder of Ag^+ ion, as suggested by conformational considerations.

Conclusions

We have reported that the new family of ***m*-C_i** formals, in analogy with the already studied ***p*-C_i** family, also behaves as a fully reversible dynamic library when treated in chloroform solution with catalytic amounts of TfOH. Information on the relative stabilities of the first three members ***m*-C_2** to ***m*-C_4** was obtained from their effective molarity values (EM_i). A comparison with the corresponding terms for the ***p*-C_i** family points to the higher stability of the ***m*-C_i** isomer, the effect being remarkably high for the dimer. We have also shown that quite reliable data on the relative stabilities of these systems can be foreseen by molecular modeling calculations. The adopted computational procedure also proved to be suitable for predicting the outcomes of cross-equilibration experiments, thus showing promise as a convenient tool for easy preliminary screening of different structures of interchangeable cyclophane formals.

Experimental Section

Instruments and General Methods: NMR spectra were recorded on either a 200 or a 300 MHz spectrometer. Chemical shifts are reported as δ values in ppm from tetramethylsilane added as an internal standard. Equilibration reactions were carried out in the NMR tube, in the thermostatted probe of the spectrometer. The experiments were run in the presence of TfOH (0.5 mM) at 25.0 °C. High-resolution mass spectra (HRMS) were performed with an Electrospray Ionisation Time of Flight Micromass spectrometer.

Materials: CF_3SO_3H was a commercial sample used without further purification. $(CF_3SO_2)_2NAg$ was prepared as described in the literature.[24] THF was dried by distillation from sodium benzophenone ketyl. $CDCl_3$ was dried with activated molecular sieves (4 Å).

Cyclic Oligomers ***m*-C_2 to ***m*-C_5: Bromochloromethane (8.28 mL, 0.135 mol) was added to a suspension of NaH (60% w/w, 5.4 g, 0.135 mol) in dry THF (450 mL). The mixture was heated to reflux, and benzene-1,3-dimethanol (3 g, 0.022 mol) in THF (50 mL) was added dropwise under argon by syringe over 24 h. The mixture was subsequently heated at reflux for two days, then cooled to room temperature, and sodium hydroxide (1 M) was added to quench the excess of NaH. After addition of water (150 mL) the mixture was extracted with CH_2Cl_2 (1 × 400 mL and 2 × 200 mL). The combined organic phases were dried with Na_2SO_4 and evaporated to give crude product (3.1 g). Pure samples of ***m*-C_2** to ***m*-C_5** were obtained by column chromatography on silica gel. After elution of a colored impurity with CH_2Cl_2/heptane 11:8, elution with CH_2Cl_2/heptane/acetone 11:8:0.7 gave the pure title compounds in the given order.

2,4,13,15-Tetraoxa[5,5]metacyclophane (*m*-C_2): White solid (300 mg, 10%); m.p. 114–115 °C. ^{1}H NMR (200 MHz, $CDCl_3$): δ = 7.30–7.29 (m, 6 H), 6.89 (s, 2 H), 4.93 (s, 4 H), 4.54 (s, 8 H) ppm. ^{13}C NMR (50 MHz, $CDCl_3$): δ = 138.52, 127.63, 128.53, 96.63, 71.01 ppm. HRMS (ESI-TOF): calcd. for $[C_{18}H_{20}O_4 + K]^+$ 339.0999; found 339.0991.

2,4,13,15,24,26-Hexaoxa[5,5,5]metacyclophane (*m*-C_3): White wax (181 mg, 6.0%). ^{1}H NMR (200 MHz, $CDCl_3$): δ = 7.41–7.29 (m, 12 H), 4.85 (s, 6 H), 4.62 (s, 12 H) ppm. ^{13}C NMR (50 MHz, $CDCl_3$): δ = 138.04, 128.65, 127.71, 127.33 94.02, 69.45 ppm. HRMS (ESI-TOF): calcd. for $[C_{27}H_{30}O_6 + K]^+$ 489.1679; found 489.1665.

2,4,13,15,24,26,35,37-Octaoxa[5,5,5,5]metacyclophane (*m*-C_4): Colorless oil (179 mg, 6.0%). ^{1}H NMR (200 MHz, $CDCl_3$): δ = 7.32–7.28 (m, 16 H), 4.83 (s, 8 H), 4.62 (s, 16 H) ppm. ^{13}C NMR (50 MHz, $CDCl_3$): δ = 138.12, 128.61, 127.38, 127.18, 94.18, 69.48 ppm. HRMS (ESI-TOF): calcd. for $[C_{36}H_{40}O_8 + Na]^+$ 623.2621; found 623.2605; calcd. for $C_{36}H_{40}O_8$+K^+ 639.2360; found 639.2382.

2,4,13,15,24,26,35,37,44,46-Decaoxa[5,5,5,5,5]metacyclophane (*m*-C_5): Colorless oil (25 mg, 0.8%). ^{1}H NMR (200 MHz, $CDCl_3$): δ = 7.36–7.28 (m, 20 H), 4.82 (s, 10 H), 4.62 (s, 20 H) ppm. ^{13}C NMR (50 MHz, $CDCl_3$): δ = 138.10, 128.58, 127.37, 127.23, 94.13, 69.43 ppm. HRMS (ESI-TOF): calcd. for $[C_{45}H_{50}O_{10} + Na]^+$ 773.3302; found 773.3319; calcd. for $[C_{45}H_{50}O_{10} + K]^+$ 789.3041; found 789.3006.

2,4,13,15-Tetraoxa[5,5]meta/paracyclophane (*m,p*-C_2): All attempts to isolate ***m,p*-C_2** as a pure sample from the equilibrated reaction mixture of the cross-transacetalation experiment failed. Purification by preparative TLC (eluent: CH_2Cl_2/heptane/acetone, 11:8:0.7) nevertheless provided a fraction containing 85% ***m,p*-C_2** and 15% ***m*-C_2**, which allowed unequivocal assignment of the ^{1}H NMR spectrum of the *cross*-dimer ***m,p*-C_2**. ^{1}H NMR (200 MHz, $CDCl_3$): δ = 7.48 (s, 4 H), 7.15–7.10 (m, 3 H), 5.45 (br s, 1 H), 4.95 (s, 4 H), 4.72 (s, 4 H), 4.35 (s, 4 H) ppm. The presence of only dimeric species $\mathbf{C_2}$ was confirmed by HRMS (ESI-TOF): calcd. for $[C_{18}H_{20}O_4 + K]^+$ 339.0999; found 339.0997.

X-ray Crystallography: Diffraction data for ***m*-C_2**, ***p*-C_2**, and ***p*-C_2** $(CF_3SO_2)_2NAg$ complex were collected with an Enraf Nonius CAD4 diffractometer with use of monochromated Cu-K_α radiation (λ = 1.54178 Å). Orientation matrices and unit cell parameters were obtained from least-squares fitting of $I(\theta,\chi,\phi)$ reflections found in random searches on the reciprocal lattices. The collected reflections were integrated and corrected for Lorentz and polarization effects. Only the data for the Ag complex were corrected for absorption by use of NEWABS92.[25] The crystal structures were solved by direct methods by use of the SIR2004 computer program[26] and refined by full-matrix, least-squares refinement by use of the SHELXL-97 computer program.[27] All non-hydrogen atoms were refined with anisotropic atomic displacements. The hydrogen atoms were included in the last cycles of the refinement with the geometrical constraint C–H 0.96 Å with a "riding" model. Geometrical calculations were obtained with PARST97.[28] Crystallographic data and the most relevant parameters for the structure refinements of ***m*-C_2**, ***p*-C_2**, and ***p*-C_2** $(CF_3SO_2)_2NAg$ are collected in Table 3.

CCDC-653071 (for ***m*-C_2**), -653072 (for ***p*-C_2**), and -653070 [for ***p*-C_2** $(CF_3SO_2)_2NAg$] contain the crystallographic data (excluding structure factors). These data can be obtained free of

Table 3. Crystallographic data and structure refinement for ***m*-C_2**, ***p*-C_2**, and ***p*-C_2** $(CF_3SO_2)_2NAg$.

	***m*-C_2**	***p*-C_2**	***p*-C_2** $(CF_3SO_2)_2NAg$
Empirical formula	$C_{18}H_{20}O_4$	$C_{18}H_{20}O_4$	$C_{18}H_{20}O_4{\cdot}(CF_3SO_2)_2NAg$
Formula weight	300.354	300.354	688.358
Crystal size [mm]	0.2 × 0.3 × 0.3	0.1 × 0.3 × 0.3	0.4 × 0.4 × 0.2
Crystal system	triclinic	triclinic	monoclinic
Space group	*P*1	*P*1	*P*2/*n*
a [Å]	10.376(5)	8.320(5)	15.747(2)
b [Å]	8.884(5)	8.445(5)	10.576(2)
c [Å]	4.378(5)	7.603(5)	16.323(2)
α [°]	83.046(5)	118.167(5)	90
β [°]	84.413(5)	66.439(5)	112.19(2)
γ [°]	71.181(5)	124.566(5)	90
V [Å^3]	378.4(5)	381.3(4)	2517.1(7)
Z	1	1	4
ρ (calcd.) [g cm^{-3}]	1.318	1.308	1.816
F(000)	160	160	1376
T [K]	295	295	295
λ [Å]	1.54178	1.54178	1.54178
μ [mm^{-1}]	0.752	0.747	8.827
Theta range [°]	3, 70	3, 70	3, 70
Reflections collected	1453	1575	5245
Independent reflections	1453 (R_{int} = 0.00)	1462 (R_{int} = 0.006)	4774 (R_{int} = 0.067)
Observed reflections	1231 $F_o \geq 4\sigma(F_o)$	1424 $F_o \geq 4\sigma(F_o)$	3352 $F_o \geq 4\sigma(F_o)$
Parameters/restraints	200/2	200/2	350/0
Goodness-of-fit on F^2 [a]	1.083	1.043	1.010
R_1	0.0351	0.0485	0.0594
wR_2	0.1187	0.1488	0.1597
Largest diff. peak and hole [e/Å^3]	0.16, –0.12	0.24, –0.28	2.30, –0.83

[a] $R_1 = \Sigma \, ||F_o| - |F_c|| / \Sigma \, |F_o|$, $wR_2 = [\Sigma w(F_o^2 - F_c^2)^2 / \Sigma w \, F_o^4]^{1/2}$. Goodness-of-fit = $[\Sigma w(F_o^2 - F_c^2)^2/(n - p)]^{1/2}$, where *n* is the number of reflections and *p* the number of parameters.

charge from The Cambridge Crystallographic Data Centre via www.ccdc.cam.ac.uk/data_request/cif.

Molecular Modeling: Molecular mechanics and molecular dynamics calculations were carried out with the MacroModel 6.0 molecular modeling system[16] running on a Silicon Graphics O2 R10000 workstation. All the calculations were carried out in vacuo, and no cut-off restrictions for the nonbonded interactions were used. The geometries were optimized to an energy gradient lower than 1×10^{-6} kJ mol^{-1} Å^{-1}, by the Polak–Ribiere conjugate gradient (PRCG) method.[29] The constant-temperature molecular-dynamics simulations were carried out without the shake algorithm and with a time step of 0.5 fs. The temperature was maintained constant with a thermal bath[30] with a bath time constant of 0.2 ps.

Supporting Information (see also the footnote on the first page of this article): Illustration of the self-assembly of two independent complex units of the $(CF_3SO_2)_2NAg$ complex of *p*-C_2 in the crystal lattice.

Acknowledgments

Financial support from Sapienza Università di Roma is acknowledged.

[1] a) P. T. Corbett, J. Leclaire, L. Vial, K. R. West, J.-L. Wietor, J. K. M. Sanders, S. Otto, *Chem. Rev.* **2006**, *106*, 3652–3711; b) N. Giuseppone, J.-M. Lehn, *Chem. Eur. J.* **2006**, *12*, 1715–1722; c) N. Giuseppone, G. Fuks, J.-M. Lehn, *Chem. Eur. J.* **2006**, *12*, 1723–1735; d) B. De Bruin, P. Hauwert, J. N. H. Reek, *Angew. Chem.* **2006**, *118*, 2726–2729; *Angew. Chem. Int. Ed.* **2006**, *45*, 2660–2663; e) P. T. Corbett, L. H. Tong, J. K. M. Sanders, S. Otto, *J. Am. Chem. Soc.* **2005**, *127*, 8902–8903; f) K. R. West, K. D. Bake, S. Otto, *Org. Lett.* **2005**, *7*, 2615–2618; g) K. C.-F. Leung, F. Aricó, S. J. Cantrill, J. F. Stoddart, *J. Am. Chem. Soc.* **2005**, *127*, 5808–5810; h) R. T. S. Lam, A. Belenguer, S. L. Roberts, C. Naumann, T. Jarrosson, S. Otto, J. K. M. Sanders, *Science* **2005**, *308*, 667–669; i) M. Horn, J. Ihringer, P. T. Glink, J. F. Stoddart, *Chem. Eur. J.* **2003**, *9*, 4046–4054; j) S. Otto, S. Kubik, *J. Am. Chem. Soc.* **2003**, *125*, 7804–7805; k) B. Fuchs, A. Nelson, A. Star, J. F. Stoddart, S. Vidal, *Angew. Chem.* **2003**, *115*, 4352–4356; *Angew. Chem. Int. Ed.* **2003**, *42*, 4220–4224; l) S. J. Rowan, S. J. Cantrill, G. R. L. Cousins, J. K. M. Sanders, J. F. Stoddart, *Angew. Chem.* **2002**, *114*, 938–993; *Angew. Chem. Int. Ed.* **2002**, *41*, 898–952; m) S. Otto, R. L. E. Furlan, J. K. M. Sanders, *Science* **2002**, *297*, 590–593; n) S. J. Rowan, D. J. Reynolds, J. K. M. Sanders, *J. Org. Chem.* **1999**, *64*, 5804–5814.

[2] a) H. A. Skinner, G. Pilcher, *Quart. Rev.* **1963**, *17*, 264–288; b) J. B. Pedley, R. D. Naylor, S. P. Kirby, *Thermochemical Data of Organic Compounds*, 2nd ed., Chapman & Hall, London, **1986**; c) J. S. Chickos, D. G. Hesse, S. Y. Panshin, D. W. Rogers, M. Saunders, P. M. Uffer, J. F. Liebman, *J. Org. Chem.* **1992**, *57*, 1897–1899.

[3] a) K. B. Wiberg, R. F. Waldron, *J. Am. Chem. Soc.* **1991**, *113*, 7697–7705; b) J. M. Brown, A. D. Conn, G. Pilcher, M. L. P. Leitão, Y. Meng-Yan, *J. Chem. Soc., Chem. Commun.* **1989**, 1817–1819; c) H. J. Rodriguez, J.-C. Chang, T. F. Thomas, *J. Am. Chem. Soc.* **1976**, *98*, 2027–2034; d) C. F. Rodriquez, I. H. Williams, *J. Chem. Soc., Perkin Trans. 2* **1997**, 953–957.

[4] See, for example: a) V. P. Vasil'ev, V. A. Borodin, S. B. Kopnyshev, *Zh. Fiz. Khim.* **1992**, *66*, 1104–1107; b) K. Byström, M. Maansson, *J. Chem. Soc., Perkin Trans. 2* **1982**, 565–569.

[5] a) R. Cacciapaglia, S. Di Stefano, L. Mandolini, *J. Am. Chem. Soc.* **2005**, *127*, 13666–13671; b) R. Cacciapaglia, S. Di Stefano, L. Mandolini, *Chem. Eur. J.* **2006**, *12*, 8566–8570.

[6] a) H. Jacobson, W. H. Stockmayer, *J. Chem. Phys.* **1950**, *18*, 1600–1606; b) G. Ercolani, L. Mandolini, P. Mencarelli, S. Roelens, *J. Am. Chem. Soc.* **1993**, *115*, 3901–3908.

[7] P. J. Flory, *Statistical Mechanics of Chain Molecules*, Wiley Interscience, New York, **1969**, Appendix D.

[8] The equilibrium constant of cyclization reaction of Equation (3) is referred to by polymer chemists as the cyclization constant (K_i). It is evident that $K_i = EM_i$ by virtue of the usual assumption that the reactivity of end groups is independent of chain length (see ref.[7]).

[9] The quantity $p^i = [\mathbf{P}_{j-i}]/[\mathbf{P}_j]$ is indistinguishable from 1 when the average length of linear species greatly exceeds *i*.

[10] a) L. Mandolini, *Adv. Phys. Org. Chem.* **1986**, *22*, 1–111; b) C. Galli, L. Mandolini, *Eur. J. Org. Chem.* **2000**, 3117–3125.

[11] It should be stressed that too much emphasis should not be placed on exact figures, because of the approximate nature of the procedure adopted to extract strain energies from experimentally measured effective molarities. More meaningful instead are differences in strain energy between isomeric rings. A reasonable expectation is that the EM^S of isomeric ***m*-C$_i$** and ***p*-C$_i$** oligomers should be identical, or very nearly so, because replacement of the *m*-phenylene units in a chain precursor such as $\mathbf{P}_i$ with *p*-phenylene units will hardly affect ΔS_{intra}. Consequently, the quantity $(\Delta E_{strain})_i$ calculated as $(\Delta E_{strain})_i = (E^{para}_{strain})_i - (E^{meta}_{strain})_i = RT\ln(EM_i^{meta}/EM_i^{para})$ is a reliable estimate of the differential strain energy between isomeric para- and metacyclophanes.

[12] G. D. Smith, R. L. Jaffe, D. Y. Yoon, *J. Phys. Chem.* **1994**, *98*, 9072–9077.

[13] This bond length was reported for a Ag^+/18-crown-6 complex. J. W. Steed, K. Johnson, C. Legido, P. C. Junk, *Polyhedron* **2003**, *22*, 769–774.

[14] $\Delta\delta$ values < 0.02 were observed for all ^{1}H NMR signals of ***m*-C$_2$** in the presence of excess solid AgOTf. In an analogous experiment $\Delta\delta$ +0.42 was observed (ref.[5a]) for the ArH signal of ***p*-C$_2$**.

[15] T. A. Halgren, *J. Comput. Chem.* **1996**, *17*, 490–519 and references cited therein.

[16] MacroModel V6.0: F. Mohamadi, N. G. J. Richards, W. C. Guida, R. Liskamp, M. Lipton, G. Chang, T. Hendrikson, W. C. Still, *J. Comput. Chem.* **1990**, *11*, 440–467.

[17] K. Gundertofte, T. Liljefors, P. Norby, I. Pettersson, *J. Comput. Chem.* **1996**, *17*, 429–449.

[18] I. Kolossváry, W. C. Guida, *J. Am. Chem. Soc.* **1996**, *118*, 5011–5019.

[19] a) G. Chang, G. Guida, W. C. Still, *J. Am. Chem. Soc.* **1989**, *111*, 4379–4386; b) M. Saunders, K. N. Houk, Y. D. Wu, W. C. Still, M. Lipton, G. Chang, W. C. Guida, *J. Am. Chem. Soc.* **1990**, *112*, 1419–1427.

[20] M. J. Engler, J. D. Andose, P. v. R. Schleyer, *J. Am. Chem. Soc.* **1973**, *95*, 8005–8025.

[21] The aromatic proton flanked by the bridges in the *meta*-substituted ring dips into the shielding cone of the *p*-phenylene nucleus. This is in agreement with the ^{1}H NMR spectrum of ***m,p*-C$_2$**, in which the signal of the given proton is significantly shifted upfield (δ = 5.45 ppm), whereas the aromatic signals of all ***m*-C$_i$** and ***p*-C$_i$** compounds are found at fields lower than 6.8 ppm.

[22] Whereas the symmetry number (σ) of ***m*-C$_2$** and ***p*-C$_2$** is 4, that of ***m,p*-C$_2$** is 2. Thus, on purely entropic grounds, the heterodimer is twice as stable as the homodimers.

[23] All attempts at obtaining ***m,p*-C$_2$** in a pure form failed. Unequivocal assignment of its ^{1}H NMR spectrum (see Exp. Sect.) was achieved by ^{1}H NMR and HRMS (ESI-TOF) analysis of a fraction from preparative TLC containing 85% of ***m,p*-C$_2$** and 15% of ***m*-C$_2$**.

[24] A. Vij, Y. Y. Zheng, R. L. Kirchmeier, J. M. Shreeve, *Inorg. Chem.* **1994**, *33*, 3281–3288.

[25] Updated version of ABSORB. See F. Ugozzoli, *Comput. Chem.* **1987**, *11*, 109–120.

[26] M. C. Burla, R. Caliandro, M. Camalli, B. Carrozzini, G. L. Cascarano, L. De Caro, C. Giacovazzo, G. Polidori, R. Spagna, *J. Appl. Crystallogr.* **2005**, *38*, 381–388.

[27] G. M. Sheldrick, SHELXL-97, *Program for Crystal Structure Refinement*, University of Göttingen, **1997**; http://shelx.uni-ac.gwdg.de/shelx/index.html.
[28] PARST97, updated version of PARST95: M. Nardelli, *J. Appl. Crystallogr.* **1995**, *28*, 659–659.
[29] E. Polak, G. Ribiere, *Rev. Fr. Rech. Oper.* **1969**, *16-R1*, 35–43.
[30] H. J. C. Berendsen, J. P. M. Postma, W. F. Van Gunsteren, A. Di Nola, J. R. Hook, *J. Chem. Phys.* **1984**, *81*, 3684–3690.
Received: September 22, 2007
Published Online: November 22, 2007

